2017

Water and nitrogen uptake are better associated with resource availability than root biomass

Peter B. Adler

esa

ECOSPHERE

Water and nitrogen uptake are better associated with resource availability than root biomass

ANDREW KULMATISKI,[1,]† PETER B. ADLER,[1] JOHN M. STARK,[2] AND ANDREW T. TREDENNICK[1]

[1]*Department of Wildland Resources, Ecology Center, Utah State University, Logan, Utah 84322 USA*
[2]*Department of Biology, Ecology Center, Utah State University, Logan, Utah 84322 USA*

Citation: Kulmatiski, A., P. B. Adler, J. M. Stark, and A. T. Tredennick. 2017. Water and nitrogen uptake are better associated with resource availability than root biomass. Ecosphere 8(3):e01738. 10.1002/ecs2.1738

Abstract. Plant uptake of soil water and nitrogen can determine plant growth, community composition, and ecosystem functioning. Despite its importance, resource uptake is typically inferred from root biomass distributions rather than measured directly. Using a depth-controlled, dual-tracer experiment, here we show that during peak growing season in a sagebrush-steppe ecosystem, vertical patterns of root biomass, water uptake, and nitrogen uptake are strikingly different from one another. Half of root biomass (0–188 cm) occurred in the top 24 cm of the soil. Half of water uptake occurred in the top 14 cm. Half of nitrogen uptake occurred in the top 79 cm. Shallow water uptake and deep nitrogen uptake were better correlated with water and nitrogen availability than with root biomass, suggesting that root systems foraged independently for different resources. Root biomass has long been used as a proxy measure of plant access to soil resources, but our results suggest that resource availability may be a better predictor of uptake.

Key words: ecohydrology; isotope; niche partitioning; nitrogen uptake; root profile; sagebrush; tracer; two-layer hypothesis; water-use.

Received 2 February 2017; accepted 3 February 2017. Corresponding Editor: Debra P. C. Peters.

† **E-mail:** andrew.kulmatiski@usu.edu

INTRODUCTION

At the cellular level, plant roots actively regulate resource uptake over time scales of hours to days (Javot and Maurel 2002, Kiba and Krapp 2016). Water and nitrogen uptake, for example, are regulated by aquaporins and nitrogen transporter proteins in fine-root membranes (Johnson et al. 2014, Kiba and Krapp 2016). The abundance and activity of these proteins can increase water and nitrogen transport several fold in response to variation in resource availability (Lauter et al. 1996, Laugier et al. 2012, Johnson et al. 2014). These results, primarily from laboratory studies, suggest that plant roots can actively, rapidly, and independently "forage" for different soil resources, but the importance of this foraging in field conditions remains largely unknown (Lauter et al. 1996, Kiba and Krapp 2016, York et al. 2016).

In the field, where resource uptake is difficult to study, uptake is often assumed to be proportional to root biomass, which itself can vary several fold in response to factors such as soil depth, competition, resource availability, and soil organisms (Lauter et al. 1996, Laugier et al. 2012, McMurtrie et al. 2012, Mueller et al. 2013, Johnson et al. 2014). This biomass-based approach largely ignores the fact that resource uptake rates may differ dramatically within a root system (Chen 2004, Hodge 2004, Göransson et al. 2007, da Silva et al. 2011, Kiba and Krapp 2016). The need for more and better data on patterns of resource uptake by plants in the field has been recognized as a key gap in understanding plant growth, species coexistence, and water and nutrient cycling (Göransson et al. 2007, Holdo 2013, Ward et al. 2013, Smithwick et al. 2014).

Here, we examine water and nitrogen uptake in a semi-arid sagebrush system in Idaho, United States. To measure patterns of soil water and nitrogen uptake, and to correlate them with root biomass, we performed a depth-controlled, dual-tracer experiment (Kulmatiski et al. 2010, da Silva et al. 2011, Mazzacavallo and Kulmatiski 2015). Injecting isotopic tracers into the soil allowed us to measure resource uptake patterns in a way that accounted for both root activity and root biomass (Gebauer and Ehleringer 2000, McKane et al. 2002, Kulmatiski et al. 2010, da Silva et al. 2011, Baudena et al. 2015, van der Heijden et al. 2015). Although tracer experiments have been used for decades, they have typically been used to examine root uptake of one element at one or two soil depths (Kirkham and Bartholomew 1954, da Silva et al. 2011, Smithwick et al. 2014, Bakhshandeh et al. 2016). Here, we measured the uptake of water and N isotopes from five specific soil depths and we compared patterns of water and nitrogen uptake to patterns of root biomass, soil water availability, and soil nitrogen availability.

Materials and Methods

Research was conducted at the U.S. Sheep Experiment Station, Dubois, Idaho, United States (Adler et al. 2012). Mean annual precipitation is 328 mm, and mean annual temperature is 6.1°C. The 2013 season, during which the experiment was performed, was drier than normal with 123 mm of precipitation compared to the long-term mean of 195 mm from the beginning of October 2012 to the beginning of June 2013. The five most common species at the site represent 86% of total plant cover. These include the shrub, *Artemisia tripartita* Rydberg (33% ± 5% of plant cover), the long-lived taprooted forb *Balsamorhiza sagittata* Hooker ex Nuttall (21% ± 5%) and the grasses *Agropyron cristatum* L. Gaertner (14% ± 4%), *Pseudoroegneria spicata* Pursh A. Love (13% ± 3%), and *Poa secunda* J. Presl (6% ± 1%). All species except *A. cristatum* are native.

Root biomass

Soil cores (5 cm wide, 83 cm deep) were taken from five randomly selected plots on 6 May, 28 May, and 19 June 2013. Sections (15 cm) were cut from the cores to determine root biomass at 10, 20, 40, and 75 cm depths. On 28 May, two soil pits were dug to 150 cm and three cores were taken from the bottom of each pit at 150 cm depths. Collected soil samples were dried to constant weight (70°C) and passed through a 2-mm mesh sieve, and all roots were collected by hand and weighed. Root biomass was calculated as the grams of dry roots divided by the grams of fine (<2 mm) dry soil. Root biomass values from 10 to 75 cm were derived from 15 different plots (n = 15), and root biomass from 150 cm was derived from six samples taken from two plots (n = 6).

Soil water and N content

Soil water and N content were measured to estimate resource availability with depth. Two methods were used to estimate soil water availability, and five methods were used to estimate soil N availability. Because water and N calculation methods produced similar estimates (Appendix S1: Fig. S1), for simplicity, we report only one estimate of water and one estimate of N availability.

Gravimetric soil water was measured in roughly 300 g, grab samples from 20, 40, 60, and 80 cm depths in three randomly selected plots in April, May, June, and July and from 150 cm depths from two soil pits in June (Appendix S1: Fig. S2). The difference in gravimetric soil water content between the beginning and end of May was used as an estimate of soil water availability. During May, 2.2 cm of precipitation occurred in daily events of 5 mm or smaller. Much of this precipitation was likely to be intercepted and evaporated before reaching surface soils (0–15 cm) which had a capacity to hold 1.7 cm of water at the beginning of May. Thus, precipitation in May was added to soil water available in the top 15 cm of soil (Inouye 2006). Our assumption that within-season precipitation would not infiltrate below 15 cm is supported from observations at a nearby study site (Inouye 2006) and results from a soil water model (Hydrus 1D) that demonstrated that even the larger precipitation events associated with the long-term precipitation patterns for the site do no not infiltrate deeper than 15 cm (Appendix S1: Fig. S3; Šimůnek et al. 2005).

To estimate extractable and available soil N, soil cores were taken from three randomly selected plots. Two, roughly 10 g subsamples from 20, 40, 60, 80, and 150 cm depths were extracted with 100 mL of 2 mol/L KCl. Extractable soil N was determined on a Lachat autoanalyzer (Lachat

Instruments, Loveland, Colorado, USA). Extractable N pools provided one estimate of soil N availability (Appendix S1: Fig. S1). However, because soil N availability is also a function of rapid N transformations in the soil (e.g., mineralization), N turnover was also calculated. Nitrogen turnover values provided an alternative estimate of N availability, but were also needed to estimate ^{15}N pool dilution and so are described in *Plant N uptake* below.

Tracer injections

Tracer injections followed the approach of Kulmatiski et al. (2010) with the exception that ^{15}N was added to the $^{2}H_2O$ water. Broadly, with this approach, we (1) injected tracers into a 15 × 15 cm grid pattern to a target depth into replicate plots, (2) measured tracer concentrations in aboveground plant tissues, and (3) for each target species, calculated the proportion of tracer uptake coming from each soil depth (Kulmatiski et al. 2010, da Silva et al. 2011, Mazzacavallo and Kulmatiski 2015). During the peak growing season (24 and 25 May 2013), 21 plots (7-m^2 circles), all separated by at least 15 m, were randomly assigned to a point located in a 4-ha area of sagebrush vegetation. Four replicate plots were assigned to each of three shallow depths (i.e., 10, 20, and 45 cm). Because deeper depths are more difficult to inject, and tend to have smaller uptake values and lower variation among values (Mazzacavallo and Kulmatiski 2015), only three replicate plots were assigned to each of the two deeper depths (i.e., 75 and 150 cm). The remaining three plots did not receive tracer injections and were used to collect "control" samples. A 15 × 15 cm grid of "pilot" holes (10 mm diameter) were created with a hammer drill (TE-60; Hilti North America, Plano, Texas, USA) to the target depth. Drilling was performed from a moveable plank system to prevent trampling of vegetation. Custom-made syringes using 16-gauge thin-walled hypodermic tubing (Vita Needle Company, Needham, Massachusetts, USA) were used to inject 1 mg $^{15}NH_4{}^{15}NO_3$ (0.34 mg N at 99 atom % ^{15}N) dissolved in 1 mL of 70% $^{2}H_2O$ into each of the 314 pilot holes in each plot. This tracer injection was immediately followed by a 2 mL tap water injection used to clear tracer from the syringe (da Silva et al. 2011). Each plot, therefore, received 942 mL or 0.13 mm of water. While injections likely resulted in a temporary and localized increase in plant available water at the point of injection, they represented roughly 2% of daily reference evapotranspiration and so were not expected to stimulate plant growth (Hargreaves and Allen 2003). Previous studies have found that the injected tracer is constrained to a roughly 10 cm depth increment by the time of plant sampling (Kulmatiski et al. 2010, Mazzacavallo and Kulmatiski 2015, Warren et al. 2015).

Plant water uptake

Two days after injections, non-transpiring tissues from the five dominant plants listed above were collected. Non-transpiring tissues were collected so that samples were not biased by evaporative enrichment at the leaf surface (Dawson and Ehleringer 1993). One to three samples, each containing plant tissues from one to several individuals, were collected with clippers that were triple-rinsed with tap water between each sample. Clipped samples were immediately sealed with paraffin wax film in custom 19-mm, medium-walled borosilicate sample tubes (Corning, New York, New York, USA) and placed on ice until moved to a freezer later in the day. Water from plant tissues was extracted by cryogenic distillation within 2 weeks (Vendramini and Sternberg 2007). Extracted water samples were analyzed for hydrogen and oxygen isotopes on a wavelength-scanned cavity ring-down spectrometer (Picarro L-2120*i;* Picarro Instruments, Santa Clara, California, USA). Isotope values (in delta notation [δ]) were converted to deuterium excess values (δ_e) to control for natural isotope enrichment caused by evaporation as follows: $\delta_e = \delta^2H - [(8 \times \delta^{18}O) + 10]$ (Gat 1996, Mazzacavallo and Kulmatiski 2015).

Plant N uptake

Three days after injections, green plant tissue samples were collected from target species in each plot. Clippers were triple-rinsed with tap water between samples. Tissues from one to several individuals were placed in paper bags, air-dried, ground, and analyzed for total N and $^{15}N/^{14}N$ ratios by continuous-flow, direct combustion, and mass spectrometry using a Europa Scientific SL-2020 (Sercon Limited, Crewe, UK).

Plant ^{15}N contents were converted to N uptake rates based on time-weighted mean ^{15}N excess calculated for soil NH_4^+ and NO_3^- pools over the

three-day experiment (Stark 2000). Predictably, extractable N pools differed with soil depth, and thus, tracer injections resulted in different ^{15}N enrichments with depth. Also N mineralization and inorganic N consumption result in dilution of the tracer over time. Because it was impossible to accurately re-sample the exact locations labeled over time (especially at the deeper depths) to measure enrichments, we estimated time-weighted mean ^{15}N enrichments of the NH_4^+ and NO_3^- pools at the labeled soil depths based on a two-compartment (NH_4^+ and NO_3^-) isotope dilution model. Initial ^{15}N enrichments were estimated from the mass of soil wet by the tracer addition (based on the measured soil water content, the amount of water added, and texture-based estimates of field capacity), soil inorganic N concentrations measured prior to injection, and the amount of ^{15}N injected. Dilution of the ^{15}N tracer was modeled assuming that turnover times of inorganic N pools were either 1 d throughout the soil or increased linearly from 1 d in the surface soil to 3 d at 150 cm (Booth et al. 2005). Separate time-weighted ^{15}N enrichments were calculated for NH_4^+ and NO_3^- pools. We assumed that plants took up NH_4^+ and NO_3^- at rates proportional to their concentrations either in KCl extracts or in the soil solution. All KCl-extractable NO_3^- was assumed to be present in the soil solution, but only a portion of extractable NH_4^+ was assumed to be water soluble (based on Stark 1991). Assumptions of one-day vs. three-day turnover times (Akaike's information criterion [AIC] = −518.0, −518.0, respectively) or N uptake based on KCl-extractable vs. water-soluble N concentrations (AIC = −1033.3, −1033.6, respectively) had minimal effects on patterns of plant N uptake (AIC values derived from generalized additive mixed-effects models [GAMMs] as described in the *Statistical analyses* section below). Because differences among calculation methods were trivial, we selected the simplest calculation method: Plant ^{15}N contents were converted to N uptake rates based on one-day turnover times and KCl-soluble NH_4^+ and NO_3^- concentrations (Stark 2000, Booth et al. 2005).

Data analyses

To allow a comparison of root biomass, ^2H uptake, ^{15}N uptake, soil water availability, and soil N availability, we standardized all values and report them as the proportion of total resource absorbed or total resource available per cm of soil depth (0–188 cm; Kulmatiski et al. 2010, Mazzacavallo and Kulmatiski 2015). This standardization also accounts for differences in tracer concentrations that can result from differences among plants in plant mass (i.e., woody plants vs. grasses) or the extent of rooting zones (i.e., plants with more roots outside the injection zone). Values were converted to proportional tracer uptake as a function of soil depth as follows:

$$\frac{S_n - C}{\sum_{n=10}^{j}(S_n - C)}$$

where S_n is the mean value of samples from treatment level n (e.g., the δ_e value of grasses at 10 cm depth in the first replicate plot). In the denominator, values (i.e., $S_n - C$) were summed across all depths from 10 to j (i.e., 10, 20, 45, 75, and 150 cm). This value was calculated for each plant species in a plot, producing three to four replicate proportion values for each plant species × depth combination. Average proportion values across species are reported to describe community-level resource uptake, and species-level data are also reported. For both community- and species-level data, cumulative proportions were calculated to identify the depth at which 50% of resource used or resource available occurred.

Statistical analyses

Our measurements of resource uptake and root biomass are discrete in space, but continuous through the soil depth profile. To approximate the continuous soil profiles of our focal variables, we fit GAMMs using a beta likelihood with a logit link for the linear predictor (soil depth). We let the GAMMs have four "knots" to allow for a smooth interpolation between the five sample depths (Appendix S1: Fig. S4). We fit nested subsets of the mixed models with different groupings of resource uptake variables and root biomass, which define each model's random-effects structure. Each group was defined a priori to represent a specific hypothesis (Tables 1 and 2); for example, root biomass is independent of water and nitrogen dynamics (model M_4 in Table 1). We fit models with group-level intercepts and slopes (the "effect" of soil depth). All models were fit in R (R Core Research Team

Table 1. Models and Akaike's information criterion (AIC) values of the distributions of root biomass, water tracer uptake, nitrogen tracer uptake, water availability, and nitrogen availability that were fit and compared.

Model	Random-effects groups	AIC
M_1	None (global model)	−769.8†
M_2	Group 1: root biomass, soil water (wu), water uptake (d)	−845.7
	Group 2: soil N (nflux), N uptake (n)	
M_3	Group 1: soil water (wu), water uptake (d)	−821.3
	Group 2: root biomass, soil N (nflux), N uptake (n)	
M_4	**Group 1: soil water (wu), water uptake (d)**	**−855.7**
	Group 2: soil N (nflux), N uptake (n)	
	Group 3: root biomass	
M_5	**Group 1: soil water (wu)**	**−855.2**
	Group 2: soil N (nflux), N uptake (n)	
	Group 3: root biomass	
	Group 4: water uptake (d)	
M_6	Group 1: soil water (wu), water uptake (d)	−846.0
	Group 2: soil N (nflux)	
	Group 3: root biomass	
	Group 4: N uptake (n)	
M_7	Group 1: soil water (wu)	−777.3
	Group 2: soil N (nflux)	
	Group 3: root biomass	
	Group 4: N uptake (n)	
	Group 5: water uptake (d)	

† The models in bold font received the most support from the data (lowest AIC).

2004) using the gam function from the mgcv package (Metadata S1; Wood 2004). We used AIC to rank models in terms of their support by the data. The model with the lowest AIC is the best model in terms of predictive ability and in terms of support from the data. Likewise, for any given hypothesis, we can compare two of the models and assess their relative support.

Niche overlap.—Niche overlap among the five species was calculated for the proportion of tracer uptake using EcoSim version 7 (Kulmatiski and Beard 2013*a*, Entsminger 2014). We used Pianka's standardized overlap value:

$$O_{jk} = \frac{\sum e_{ij} e_{ik}}{\sqrt{\sum e_{ij}^2 e_{ik}^2}}$$

where O_{jk} is a measure of overlap between species j and k, the electivity index $e_{ij} = p_{ij}/R_j$, where p_{ij} is the proportion that resource i is of the total resource used by species j, p_{ik} is the proportion that resource i is of the total resources used by species k, and R_j is a measure of the availability of resource state j (Singh et al. 2013). This unitless measure ranges from 0 to 1, where 0 indicates complete niche separation. To determine whether observed overlap values were likely to result by chance, the species utilization matrices were compared to predictions from a randomized null model. Randomization algorithm three in EcoSim version 7 (Acquired Intelligence, Inc., Montrose, Colorado, USA), in which niche breadth is retained and zero states are reshuffled, was used because niche breadth did appear to differ by species, zero uptake did not appear to be a fixed species trait for any depth (i.e., all plants accessed some tracer from every depth sampled during one time period or another), and this approach is usually superior in detecting non-random overlap (Winemiller and Pianka 1990). In this experiment, zero states would be depths from which a plant does not access soil water or nitrogen.

Table 2. Models and Akaike's information criterion (AIC) values of the distribution of either water uptake or nitrogen uptake for the five target species in the experiment that were fit and compared.

Model	Random-effects groups	AIC (water)	AIC (N)
M_1	None (global model)	−592.9	**−131.9**†
M_2	Group 1: Grasses (AC, PS, PSSP)	**−631.8**	**−131.8**
	Group 2: Woody (AT, BS)		
M_3	Group 1: Native grasses (PS, PSSP)	**−631.8**	**−131.8**
	Group 2: Non-native grass (AC)		
	Group 3: Woody (AT, BS)		
M_4	Group 1: Shrub (AT)	−592.6	**−131.8**
	Group 2: Forb (BS)		
	Group 3: Grass (AC, PS, PSSP)		
M_5	Group 1: AC	**−631.8**	**−131.8**
	Group 2: AT		
	Group 3: BS		
	Group 4: PS		
	Group 5: PSSP		

AC, *Agropyron cristatum*; AT, *Artemisia tridentata*; BS, *Balsamorhiza sagittata*; PS, *Poa secunda*; PSSP, *Pseudoroegneria spicata*.

† The AIC values in bold face received the most support from the data (lowest AIC).

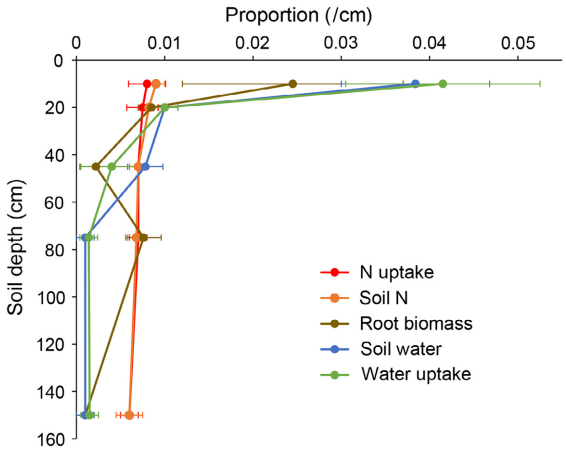

Fig. 1. Root biomass, H_2O uptake, N uptake, soil water available, and soil nitrogen available with depth. Generalized additive mixed-effects models used to describe these distributions indicated that water and nitrogen uptake differed from each other and were more similar to water and nitrogen availability than root biomass. Values are the proportion of resource used or resource available per cm of soil depth (0–188 cm). Data points represent mean values, and error bars indicate minimum and maximum values.

Results

Root biomass decreased from a maximum of 2.5%/cm at the surface to a minimum of 0.04%/cm at 188 cm (Fig. 1). The cumulative proportion of root biomass with depth indicated that 50% of root biomass occurred above 24 cm. Water uptake was shallower (Fig. 1): 50% of ^2H_2O uptake occurred above 14 cm. This distribution of water uptake was similar to the distribution of water available: 50% of available soil moisture occurred above 15 cm (Fig. 1). Nitrogen uptake was deeper than either water uptake or root biomass (Fig. 1): 50% of ^{15}N was absorbed above 86 cm. The distribution of N uptake was similar to the distribution of N availability: 50% of available N occurred above 84 cm (Fig. 1).

When GAMMs were used to approximate the continuous soil profiles of root biomass, water uptake, N uptake, soil water available, and soil N flux, the best model grouped N uptake with N flux, grouped water uptake with soil water available, and separated root biomass, but this model was statistically indistinguishable from a model that only grouped N uptake with N concentration and separated the remaining profiles (Fig. 1, Table 1). Models that combined root biomass with water uptake or root biomass with N uptake did not perform as well (Fig. 1, Table 1). In other words, the pattern of water uptake was more similar to the pattern of water availability than to the patterns of root biomass or N uptake. Similarly, N uptake was more similar to N availability than to root biomass or water uptake. More broadly, these models indicated that resource uptake was more consistent with resource availability than root biomass.

For water uptake by species, three models were equally supported: the model that separated all profiles, the model that separated grasses and woody plants, and the model that separated woody plants from native grass and the non-native grass (Fig. 2A, Table 2). Model differences reflected large surface water uptake by *Poa secunda,* large medium depth uptake (i.e., 20–45 cm) by *Pseudoroegneria spicata*, and large deep uptake (i.e., 75–150 cm) by *Artemisia tridentata.* Fifty percent of water uptake occurred above 20, 13, 13, 11, and 9 cm, for *A. tridentata, Artemisia cristata, P. spicata, Balsamorhiza sagittata*, and *P. secunda,* respectively.

For N uptake by species, there was no difference among models (Fig. 2B, Table 2). This reflected complex patterns or high variability in N uptake with depth. Differences in N uptake among species reflected large surface N uptake by *P. secunda* and *P. spicata* and large deep N uptake (75 and 150 cm) by *Agropyron cristatum, A. tridentata,* and *B. sagittata* (Fig. 2B, Table 2). Fifty percent of N uptake occurred above 87, 82, 81, 64, and 61 cm for *A. cristata, A. tridentata, B. sagittata, P. spicata*, and *P. secunda,* respectively.

Despite differences in water and N uptake profiles among species, niche overlap in water uptake (0.94) and N uptake (0.86) was very large though not greater than would be expected by chance (P = 0.09 and 0.11, respectively).

Discussion

At the plant community level, we found striking differences among the distributions of root biomass, water uptake, and N uptake with depth. Water uptake was shallower than would be predicted from root biomass, but consistent with water availability. A likely explanation for shallow water uptake is that plants increased

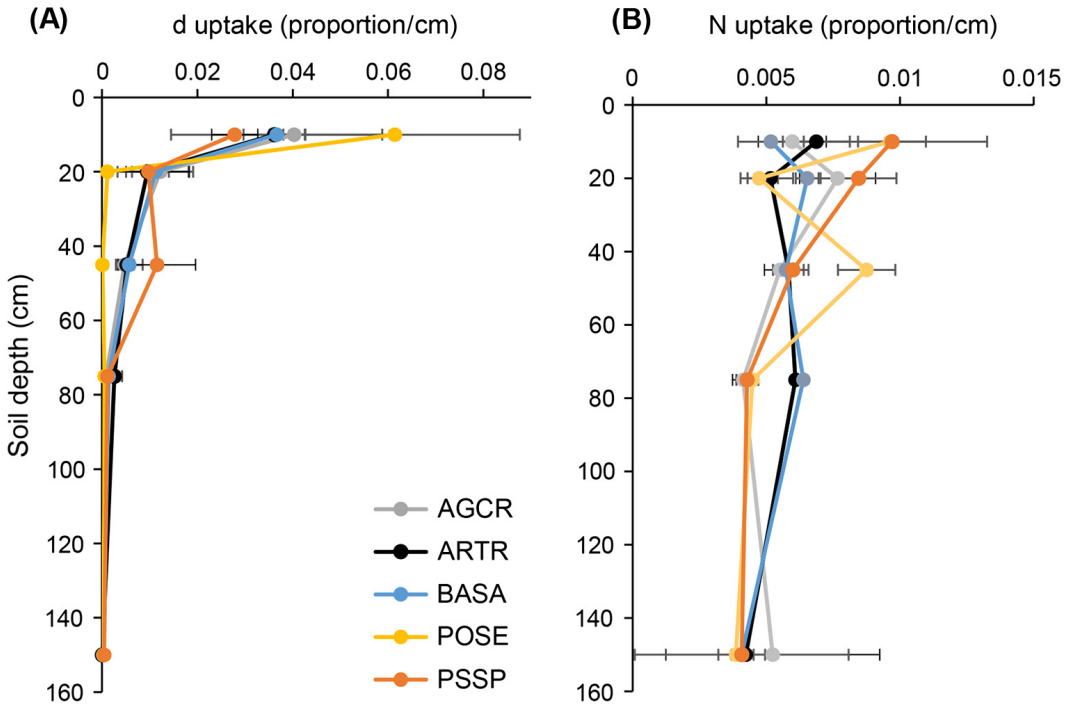

Fig. 2. The proportion of (A) water (d) and (B) nitrogen (N) tracer uptake by depth for five dominant plant species. Tracers were injected to the indicated target soil depths in three (75–150 cm) to four (10–45 cm) replicate plots. The amount of tracer in a sample was divided by the sum of tracer uptake across depths to calculate the proportion of uptake by depth. Standard errors associated with variation among the three to four replicate plots are reported. Note the different scale on the *x*-axis between plots.

aquaporin abundance or activity in shallow soils in response to greater water availability in shallow soils (Javot and Maurel 2002, Hodge 2004, Johnson et al. 2014, van der Heijden et al. 2015). In contrast to water uptake, N uptake was deeper than suggested by root biomass, but consistent with soil N availability. A likely explanation for deep N uptake is that plants increased N transporter protein abundance or activity in deep roots in response to soil N availability (Lauter et al. 1996, Johnson et al. 2014, Kiba and Krapp 2016, York et al. 2016). Interestingly, the root biomass profile was between the water and N uptake profiles, suggesting that root biomass allocation balanced demands for water and N.

Researchers working at the cellular level have long recognized that plants can modify resource uptake in response to resource availability (Lauter et al. 1996, Javot and Maurel 2002), yet the extent of this effect in field conditions remains largely unknown because most field-based research has measured root biomass as a proxy for uptake (Göransson et al. 2007, McMurtrie et al. 2012, Holdo 2013, Smithwick et al. 2014, Baudena et al. 2015). Our results, from a field experiment, demonstrated that water and N uptake profiles can differ from each other and from root biomass profiles in a pattern that is consistent with resource availability. Similar results have been found for other elements, typically at one or two soil depths, but our research focuses on two primary limiting resources and documents uptake at five specific soil depths (Gebauer and Ehleringer 2000, McKane et al. 2002, Kulmatiski et al. 2010, da Silva et al. 2011, van der Heijden et al. 2015).

Soil nitrogen is most abundant near the soil surface leading to the suggestion that plant root abundance should be greatest near the surface (Ryel et al. 2008, Schenk 2008, February and Higgins 2010). While we found that N uptake was surprisingly deep relative to root biomass and water uptake, we did observe that soil N and soil N uptake were both greatest near the surface. Our results highlight the fact that soil N tends to

decrease with depth more slowly than soil resources such as soil water or soil carbon (Kulmatiski et al. 2004, Yang et al. 2010).

Results at the species level were consistent with results at the community level. While there were differences in uptake profiles among species, all plants demonstrated deeper N uptake profiles than water uptake profiles. The similarity in either water or N uptake profiles resulted in very large niche overlap among species for both water and N uptake. Research with long-term data sets and models at our site shows that population growth is more limited by intra- than interspecific interactions, strongly stabilizing coexistence (Adler et al. 2012). One potential explanation of these dynamics would be partitioning of soil resources by depth, but our results suggest that peak-season niche partitioning was not a likely explanation of species coexistence, at least during the relatively dry year of the experiment.

While niche overlap was large in this experiment, differences in resource uptake were detectable. Not surprisingly, the two long-lived woody native species *Artemisia tridentata* and *Balsamorhiza sagittata* demonstrated deeper water and N uptake profiles than the two native grasses. Interestingly, these two native woody species, with notably deeper rooting, were also the most abundant in the community. The deeper uptake profile of the two woody plants is consistent with Walter's two-layer hypothesis (Ward et al. 2013) and the related two-pool hypothesis (Ryel et al. 2008, Germino and Reinhardt 2014, Prieto and Ryel 2014, Roundy et al. 2014), but again, this support is weak because niche overlap was very large. The non-native grass *Agropyron cristatum* demonstrated surprisingly deep root uptake of both water and N, especially when compared to the two native grasses.

Conclusions about niche partitioning of soil resources must be taken with caution because they were derived from one mid-season sampling in a dry year. Similar experiments, repeated over time, are needed to better understand resource uptake and partitioning (Volkmann et al. 2016). Studies that have examined water uptake over time have found that some, particularly woody, plants shift resource uptake profiles within growing seasons (Chen 2004, Kulmatiski et al. 2010, Kulmatiski and Beard 2013*a*, Volkmann et al. 2016).

The active and independent "foraging" for soil water and N observed in this study has implications for plant growth, species coexistence, and the cycling of water, energy, and nutrients (McKane et al. 2002, Mueller et al. 2013, Baudena et al. 2015). Our results provided mixed support for contrasting perspectives on root dynamics such as the two-layer (Ward et al. 2013), or two-pool hypotheses (Ryel et al. 2008). Rather than testing general hypotheses about root dynamics, we suggest that an important direction for future research will be to use tracer uptake data to model plant growth and water cycling over many growing seasons (Peters 2002, McMurtrie et al. 2012, Mazzacavallo and Kulmatiski 2015). For example, the data produced here can be used in plant growth and ecohydrological models to estimate plant growth and competition as well as water cycling at different sites and under different hydrological conditions (Peters 2002, Schymanski et al. 2009, Kulmatiski and Beard 2013*b*, Mazzacavallo and Kulmatiski 2015).

Acknowledgments

This research was supported by the Utah Agricultural Experiment Station, Utah State University, and approved as journal paper number 8946. Thanks to the U.S. Sheep Experiment Station for use of their land and housing and to Marina LaForgia, Carlee Coleman, and Andy Kleinhesselink for help in the field. AK was supported by an NSF Division of Environmental Biology Award (DEB—1354129). ATT was supported by an NSF Postdoctoral Fellowship in Biology (DBI-1400370).

Literature Cited

Adler, P. B., H. J. Dalgleish, and S. P. Ellner. 2012. Forecasting plant community impacts of climate variability and change: When do competitive interactions matter? Journal of Ecology 100:478–487.

Bakhshandeh, S., M. A. Kertesz, P. E. Corneo, and F. A. Dijkstra. 2016. Dual-labeling with ^{15}N and $H_2{}^{18}O$ to investigate water and N uptake of wheat under different water regimes. Plant and Soil 408:429–441.

Baudena, M., et al. 2015. Forests, savannas, and grasslands: bridging the knowledge gap between ecology and Dynamic Global Vegetation Models. Biogeosciences 12:1833–1848.

Booth, M. S., J. M. Stark, and E. Rastetter. 2005. Controls on nitrogen cycling in terrestrial ecosystems: a synthetic analysis of literature data. Ecological Monographs 75:139–157.

Chen, X. Y. 2004. Seasonal patterns of fine-root productivity and turnover in a tropical savanna of

northern Australia. Journal of Tropical Ecology 20: 221–224.

da Silva, E. V., J. P. Bouillet, J. L. de Moraes Gonçalves, C. H. A. Junior, P. C. O. Trivelin, P. Hinsinger, C. Jourdan, Y. Nouvellon, J. L. Stape, and J. P. Laclau. 2011. Functional specialization of Eucalyptus fine roots: contrasting potential uptake rates for nitrogen, potassium and calcium tracers at varying soil depths. Functional Ecology 25:996–1006.

Dawson, T. E., and J. R. Ehleringer. 1993. Isotopic enrichment of water in the woody tissues of plants—implications for plant water source, water-uptake, and other studies which use the stable isotopic composition of cellulose. Geochimica et Cosmochimica Acta 57:3487–3492.

Entsminger, G. L. 2014. EcoSim Professional: null modelling software for ecologists, Version 1. Acquired Intelligence, Inc. & Kesey-Bear, Montrose, Colorado, USA.

February, E. C., and S. I. Higgins. 2010. The distribution of tree and grass roots in savannas in relation to soil nitrogen and water. South African Journal of Botany 76:517–523.

Gat, J. R. 1996. Oxygen and hydrogen isotopes in the hydrologic cycle. Annual Review of Earth and Planetary Sciences 24:225–262.

Gebauer, R. L. E., and J. R. Ehleringer. 2000. Water and nitrogen uptake patterns following moisture pulses in a cold desert community. Ecology 81:1415–1424.

Germino, M. J., and K. Reinhardt. 2014. Desert shrub responses to experimental modification of precipitation seasonality and soil depth: relationship to the two-layer hypothesis and ecohydrological niche. Journal of Ecology 102:989–997.

Göransson, H., A.-M. Fransson, and U. Jönsson-Belyazid. 2007. Do oaks have different strategies for uptake of N, K and P depending on soil depth? Plant and Soil 297:119–125.

Hargreaves, G. H., and R. G. Allen. 2003. History and evaluation of Hargreaves evapotranspiration equation. Journal of Irrigation and Drainage Engineering 129:53–63.

Hodge, A. 2004. The plastic plant: root responses to heterogeneous supplies of nutrients. New Phytologist 162:9–24.

Holdo, R. M. 2013. Revisiting the two-layer hypothesis: coexistence of alternative functional rooting strategies in savannas. PLoS ONE 8:e69625.

Inouye, R. S. 2006. Effects of shrub removal and nitrogen addition on soil moisture in sagebrush steppe. Journal of Arid Environments 65:604–618.

Javot, H., and C. Maurel. 2002. The role of aquaporins in root water uptake. Annals of Botany 90:301–313.

Johnson, D. M., M. E. Sherrard, J.-C. Domec, and R. B. Jackson. 2014. Role of aquaporin activity in regulating deep and shallow root hydraulic conductance during extreme drought. Trees 28: 1323–1331.

Kiba, T., and A. Krapp. 2016. Plant Nitrogen Acquisition Under Low Availability: Regulation of Uptake and Root Architecture. Plant Cell Physiology 57:707–714.

Kirkham, D., and W. Bartholomew. 1954. Equations for following nutrient transformations in soil, utilizing tracer data. Soil Science Society of America Journal 18:33–34.

Kulmatiski, A., and K. H. Beard. 2013*a*. Root niche partitioning among grasses, saplings, and trees measured using a tracer technique. Oecologia 171: 25–37.

Kulmatiski, A., and K. H. Beard. 2013*b*. Woody plant encroachment facilitated by increased precipitation intensity. Nature Climate Change 3:833–837.

Kulmatiski, A., K. H. Beard, R. J. T. Verweij, and E. C. February. 2010. A depth-controlled tracer technique measures vertical, horizontal and temporal patterns of water use by trees and grasses in a subtropical savanna. New Phytologist 188:199–209.

Kulmatiski, A., D. J. Vogt, T. G. Siccama, J. P. Tilley, K. Kolesinskas, T. W. Wickwire, and B. C. Larson. 2004. Landscape determinants of soil carbon and nitrogen storage in southern New England. Soil Science Society of America Journal 68:2014–2022.

Laugier, E., E. Bouguyon, A. Mauriès, P. Tillard, A. Gojon, and L. Lejay. 2012. Regulation of high-affinity nitrate uptake in roots of Arabidopsis depends predominantly on posttranscriptional control of the NRT2. 1/NAR2. 1 transport system. Plant Physiology 158:1067–1078.

Lauter, F.-R., O. Ninnemann, M. Bucher, J. W. Riesmeier, and W. B. Frommer. 1996. Preferential expression of an ammonium transporter and of two putative nitrate transporters in root hairs of tomato. Proceedings of the National Academy of Sciences 93:8139–8144.

Mazzacavallo, M. G., and A. Kulmatiski. 2015. Modelling water uptake provides a new perspective on grass and tree coexistence. PLoS ONE 10:e0144300.

McKane, R. B., et al. 2002. Resource-based niches provide a basis for plant species diversity and dominance in arctic tundra. Nature 415:68–71.

McMurtrie, R. E., C. M. Iversen, R. C. Dewar, B. E. Medlyn, T. Näsholm, D. A. Pepper, and R. J. Norby. 2012. Plant root distributions and nitrogen uptake predicted by a hypothesis of optimal root foraging. Ecology and Evolution 2:1235–1250.

Mueller, K. E., D. Tilman, D. A. Fornara, and S. E. Hobbie. 2013. Root depth distribution and the diversity-productivity relationship in a long-term grassland experiment. Ecology 94:787–793.

Peters, D. P. C. 2002. Plant species dominance at a grassland-shrubland ecotone: an individual-based gap dynamics model of herbaceous and woody species. Ecological Modelling 152:5–32.

Prieto, I., and R. J. Ryel. 2014. Internal hydraulic redistribution prevents the loss of root conductivity during drought. Tree Physiology 34:39–48.

R Core Research Team. 2004. R: a language and environment for statistical computing. R Foundation for Statistical Computing, Vienna, Austria. http://www.R-project.org/

Roundy, B. A., R. F. Miller, R. J. Tausch, K. Young, A. Hulet, B. Rau, B. Jessop, J. C. Chambers, and D. Eggett. 2014. Understory cover responses to pinon–juniper treatments across tree dominance gradients in the Great Basin. Rangeland Ecology and Management 67:482–494.

Ryel, R. J., C. Y. Ivans, M. S. Peek, and A. J. Leffler. 2008. Functional differences in soil water pools: a new perspective on plant water use in water-limited ecosystems. Pages 397–422 *in* U. Luttge, W. Beyschlag, and J. Murata, editors. Progress in botany. Springer, Berlin, Germany.

Schenk, H. J. 2008. The shallowest possible water extraction profile: a null model for global root distributions. Vadose Zone Journal 7:1119–1124.

Schymanski, S. J., M. Sivapalan, M. L. Roderick, L. B. Hutley, and J. Beringer. 2009. An optimality-based model of the dynamic feedbacks between natural vegetation and the water balance. Water Resources Research 45:W01412.

Šimůnek, J., M. Šejna, H. Saito, M. Sakai, and M. T. Van Genuchten. 2005. The HYDRUS-1D software package for simulating the one-dimensional movement of water, heat, and multiple solutes in variably-saturated media, Version 4.17. Hydrus Software Series 3, University of California-Riverside Research Reports, Riverside, California, USA. Pages 1–342.

Singh, D., M. Tsiang, B. Rajaratnam, and N. S. Diffenbaugh. 2013. Precipitation extremes over the continental United States in a transient, high-resolution, ensemble climate model experiment. Journal of Geophysical Research: Atmospheres 118:7063–7086.

Smithwick, E. A. H., M. S. Lucash, M. L. McCormack, and G. Sivandran. 2014. Improving the representation of roots in terrestrial models. Ecological Modelling 291:193–204.

Stark, J. M. 1991. Environmental factors versus ammonia-oxidizer population characteristics as dominant controllers of nitrification in an oak woodland-annual grassland soil. University of California, Berkeley, California, USA.

Stark, J. M. 2000. Nutrient transformations. Pages 215–234 *in* O. E. Sala, R. B. Jackson, H. A. Mooney, and R. W. Howarth, editors. Methods in ecosystem science. Springer-Verlag, New York, New York, USA.

van der Heijden, G., E. Dambrine, B. Pollier, B. Zeller, J. Ranger, and A. Legout. 2015. Mg and Ca uptake by roots in relation to depth and allocation to aboveground tissues: results from an isotopic labeling study in a beech forest on base-poor soil. Biogeochemistry 122:375–393.

Vendramini, P. F., and L. Sternberg. 2007. A faster plant stem-water extraction method. Rapid Communications in Mass Spectrometry 21:164–168.

Volkmann, T. H., K. Haberer, A. Gessler, and M. Weiler. 2016. High-resolution isotope measurements resolve rapid ecohydrological dynamics at the soil–plant interface. New Phytologist 210:839–849.

Ward, D., K. Wiegand, and S. Getzin. 2013. Walter's two-layer hypothesis revisited: back to the roots! Oecologia 172:617–630.

Warren, C. P., A. Kulmatiski, and K. H. Beard. 2015. A combined tracer/evapotranspiration model approach estimates plant water uptake in native and non-native shrub-steppe communities. Journal of Arid Environments 121:67–78.

Winemiller, K. O., and E. R. Pianka. 1990. Organization in natural assemblages of desert lizards and tropical fishes. Ecological Monographs 60:27–55.

Wood, S. N. 2004. Stable and efficient multiple smoothing parameter estimation for generalized additive models. Journal of the American Statistical Association 99:673–686.

Yang, Y., J. Fang, D. Guo, C. Ji, and W. Ma. 2010. Vertical patterns of soil carbon, nitrogen and carbon: nitrogen stoichiometry in Tibetan grasslands. Biogeosciences Discussions 7:1–24.

York, L. M., M. Silberbush, and J. P. Lynch. 2016. Spatiotemporal variation of nitrate uptake kinetics within the maize (*Zea mays* L.) root system is associated with greater nitrate uptake and interactions with architectural phenes. Journal of Experimental Botany 67:3763–3775.

Supporting Information

Additional Supporting Information may be found online at: http://onlinelibrary.wiley.com/doi/10.1002/ecs2.1738/full